
Semiautomatic Tumor Delineation for Evaluation of ^{64}Cu -DOTATATE PET/CT in Patients with Neuroendocrine Neoplasms: Prognostication Based on Lowest Lesion Uptake and Total Tumor Volume

Esben Andreas Carlsen^{1,2}, Camilla Bardram Johnbeck^{1,2}, Mathias Loft^{1,2}, Andreas Pfeifer^{1,2}, Peter Oturai^{1,2}, Seppo W. Langer^{2,3}, Ulrich Knigge^{2,4}, Claes Nøhr Ladefoged^{*1,2}, and Andreas Kjaer^{*1,2}

¹Department of Clinical Physiology, Nuclear Medicine & PET and Cluster for Molecular Imaging, Department of Biomedical Sciences, Rigshospitalet and University of Copenhagen, Copenhagen, Denmark; ²ENETS Neuroendocrine Tumor Center of Excellence, Rigshospitalet, Copenhagen, Denmark; ³Department of Oncology, Rigshospitalet, Copenhagen, Denmark; and ⁴Departments of Clinical Endocrinology and Surgical Gastroenterology, Rigshospitalet, Copenhagen, Denmark

J Nucl Med 2021; 62:1564–1570

DOI: 10.2967/jnumed.120.258392

Patients with neuroendocrine neoplasms (NENs) have heterogeneous somatostatin receptor expression, with highly differentiated lesions having higher expression. Receptor expression of the total tumor burden may be visualized by somatostatin receptor imaging, such as with ^{64}Cu -DOTATATE PET/CT. Assessment of maximal lesion uptake is associated with progression-free survival (PFS) but not overall survival (OS). We hypothesized that the lesion with the lowest, rather than the highest, ^{64}Cu -DOTATATE uptake would be more prognostic, and we developed a semiautomatic method for evaluating this hypothesis.

Methods: Patients with NENs underwent ^{64}Cu -DOTATATE PET/CT. A standardized semiautomatic tumor delineation method was developed and used to identify the lesion with the lowest uptake, that is, with the lowest SUV_{mean} . Additionally, we assessed total tumor volume derived from the semiautomatic tumor delineation. Kaplan–Meier and Cox regression analyses were used to determine whether there was any association with OS and PFS. **Results:** In 116 patients with NENs, median PFS (95% CI) was 23 mo (range, 20–31 mo) and median OS was 85 mo (range, 68–113 mo). Minimum SUV_{mean} and total tumor volume were significantly associated with PFS and OS in univariate Cox regression analyses, whereas SUV_{max} was significant only for PFS. In multivariate Cox analyses, both minimum SUV_{mean} and total tumor volume remained statistically significant. Minimum SUV_{mean} and total tumor volume were then dichotomized by their median, and patients were categorized into 4 groups: high or low total tumor volume and high or low minimum SUV_{mean} . Patients with a low total tumor volume and high minimum SUV_{mean} had a hazard ratio of 0.32 (95% CI, 0.20–0.51) for PFS and 0.24 (95% CI, 0.13–0.43) for OS, both with P values of less than 0.001 (reference: high total tumor volume and low minimum SUV_{mean}). **Conclusion:** We propose a standardized semiautomatic tumor delineation method to identify the lesion with the lowest ^{64}Cu -DOTATATE uptake and total tumor volume. Assessment of the lowest, rather than the highest, lesion uptake greatly increases prognostication by ^{64}Cu -DOTATATE PET/CT. Combining lesion uptake and total tumor volume, we derived a novel prognostic classification system for patients with NENs.

Key Words: neuroendocrine neoplasms; ^{64}Cu -DOTATATE PET; semiautomatic tumor delineation; minimum SUV_{mean} ; total tumor volume

Patients with neuroendocrine neoplasms (NENs) have a disease course and survival span that vary considerably. In recent years, several treatment options have been validated for patients with NENs. One criterion that can be used to select different treatment strategies is the expected prognosis of a patient, that is, more aggressive treatment in patients with a rapid and aggressive disease course. In patients with NENs, the World Health Organization grading scheme based on the proliferation marker Ki-67 determined either in a biopsy or in a surgically resected tumor presently plays a crucial role in this regard. Currently, NEN patients are graded according to Ki-67 and tumor differentiation (1). However, a known limitation is interlesional tumor heterogeneity between primary tumor and metastatic lesions (2–5). Furthermore, with disease progression, an increase in Ki-67 is seen (4). Sampling of the entire tumor or several lesions frequently shows an increase in Ki-67 and World Health Organization grade (2–5). Hence, prediction of prognosis may be enhanced by assessing the total tumor volume to identify the most dedifferentiated lesion. This assessment, as well as longitudinal monitoring, is possible using whole-body PET assessment.

PET is widely used in patients with NENs, especially somatostatin receptor imaging (SRI) by radiolabeled somatostatin analogs, such as ^{64}Cu -DOTATATE, ^{68}Ga -DOTATATE, or ^{68}Ga -DOTA-TOC in patients with low-grade NENs, and glucose uptake imaging by ^{18}F -FDG in patients with high-grade NENs. We have previously reported the ability of ^{64}Cu -DOTATATE PET to predict overall survival (OS) and progression-free survival (PFS) in patients with NENs (6). Although unable to identify a cutoff to predict OS, we showed that patients with a tumor SUV_{max} of more than 43.3 had half the risk of progressive disease, compared with patients with an SUV_{max} of 43.3 or less. The highest tumor SUV_{max} for a patient is easy to obtain; however, it reflects the greatest somatostatin receptor density and therefore the prediction is likely based on the most differentiated, and least aggressive, tumor area. For ^{18}F -FDG PET, both metabolic tumor volume and total lesion glycolysis have been reported (7–9), and these measures have also been adopted

Received Oct. 14, 2020; revision accepted Feb. 3, 2021.

For correspondence or reprints, contact Andreas Kjaer (akjaer@sund.ku.dk).

*Contributed equally to this work.

Published online February 26, 2021.

COPYRIGHT © 2021 by the Society of Nuclear Medicine and Molecular Imaging.

for SRI (10). Total tumor volume based on SRI tumor segmentation has been shown to have prognostic implications (11–14). Besides volumetric information, the lowest lesion SUV_{mean} would also be available with total tumor segmentation, and thus, the most dedifferentiated lesion could be used for prognostication.

The aim of this paper is to propose a scheme for semiautomated tumor delineation in ^{64}Cu -DOTATATE PET for patients with NENs and to use this scheme to improve the prognostic value of ^{64}Cu -DOTATATE. To do so, measures of the lowest lesion SUV_{mean} and total tumor volume extracted from tumor delineation were used. We hypothesized that this scheme could increase the prognostic value of ^{64}Cu -DOTATATE PET compared with the previously reported method based on SUV_{max} .

MATERIALS AND METHODS

Patients

Between November 2009 and March 2013, our group recruited patients with NENs in 2 prospective clinical studies with ^{64}Cu -DOTATATE PET/CT (15,16), approved by the Regional Scientific Ethical Committee (reference no. H-D-2008-045). Written informed consent was obtained from all participants. The included patients had histopathologically confirmed gastroenteropancreatic or lung NENs or NENs of unknown primary and were referred for PET/CT for staging, restaging, or follow-up. All scans were reviewed for inclusion in the present follow-up study. If more than one ^{64}Cu -DOTATATE PET/CT exam was available for a patient, the earliest scan was used. We excluded patients with no signs of NENs because of previous radical surgery. Patients were followed and treated with the standard of care at the ENETS Neuroendocrine Tumor Center of Excellence, Rigshospitalet, Copenhagen, Denmark. Treatment decisions were made by multidisciplinary tumor boards masked to the ^{64}Cu -DOTATATE PET/CT findings but guided by ^{111}In -octreotide scintigraphy (clinical routine throughout the inclusion period), Ki-67, World Health Organization grade, and tumor location. Patient characteristics collected at baseline were age, sex, site of primary tumor, Ki-67 index (%), grade, and treatment. The patients were assessed at regular follow-up visits and with diagnostic CT performed according to guidelines (17). At the discretion of the treating physician, SRI, MRI, or ultrasound was also performed during follow-up.

Radiotracer and Image Acquisition

Radiotracer production, PET/CT image acquisition, and reconstruction methodology have been published previously (15,16,18). In short, patients underwent whole-body PET/CT at 61 ± 1 min (range, 43–99 min) after injection of 202 ± 1 MBq (range, 174–245 MBq) of ^{64}Cu -DOTATATE. A Siemens Biograph 40 or 64 TruePoint PET/CT scanner was used. All images were reconstructed with the same algorithm (TrueX; Siemens Medical Solutions) using 3 iterations and 21 subsets and smoothed by 2-mm gaussian filter (full width at half maximum), on 336×336 matrices ($2 \times 2 \times 3$ mm voxels). CT-based attenuation correction was applied. A diagnostic-quality CT scan with iodine intravenous contrast medium was performed before the PET. If contraindicated, iodine contrast was not used. To ensure quantitatively accurate measurements between the different PET/CT scanners, we perform a quality control every 2 wk, testing whether they are calibrated to within our acceptance range (5%).

Image Analysis

All PET/CT scans were analyzed using the DBx software package (version 1.2.0; Mirada Medical Ltd.) masked to the patients' PFS and OS. A nuclear medicine physician in training analyzed all scans, and a subgroup ($n = 12$) was additionally assessed by a board-certified nuclear medicine physician masked to the results of the former. To the best of our

knowledge, no standardized method for semiautomated tumor delineation using SRI PET has been proposed. We therefore adapted the method proposed in PERCIST for ^{18}F -FDG PET to obtain a standardized patient-specific threshold of $(1.5 \times \text{liver } SUV_{mean}) + (2 \times \text{SD})$ (19). Lower thresholds increase the delineation of lesions with a low tracer uptake but also increase physiologic tracer uptake, which would substantially limit the semiautomated approach. According to PERCIST, if no normal liver is available (e.g., full cancer involvement), the blood value should be used. However, in SRI PET, the blood value is markedly lower than the liver. We therefore chose to use normal spleen uptake when normal liver tissue could not be assessed. In each patient, a 3-cm sphere was placed in normal liver tissue (or in normal spleen tissue). SUV_{mean} and SD were extracted and used to calculate the patient-specific threshold by the following formula:

$$\text{Liver: } (1.5 \times SUV_{mean}) + (2 \times \text{SD})$$

This formula was adapted for spleen SUV_{mean} on the basis of normal data available in a previous publication (20):

$$\text{Spleen: } (0.67 \times SUV_{mean}) + (2 \times \text{SD})$$

SUV was calculated as decay-corrected measured radioactivity concentration/(injected activity/body weight). A region encompassing all lesions was then drawn manually, and voxels with an SUV above the threshold were delineated automatically. Delineated noise (i.e., nonpathologic tracer uptake) and physiologic tracer uptake (pituitary gland, liver, spleen, kidneys, adrenal glands, urinary tract, and uncinate process of pancreas) was manually deleted.

Data Extraction

The partial-volume effect results in an underestimation of SUV in small lesions. We therefore defined a minimum lesion size of 1 cm^3 because the partial-volume effect typically occurs in lesions smaller than 3 times the full width at half maximum (21). To obtain the minimum SUV_{mean} (i.e., the lesion with the lowest SUV_{mean}), data were extracted for each lesion individually. Confluent lesions were considered as one if the lesions were not separated on the basis of the patient-specific threshold. Furthermore, total tumor volume (i.e., the sum of all lesions) was derived from the ^{64}Cu -DOTATATE PET images.

Endpoints

Follow-up was performed on July 13, 2020. CT routine images or MR images were used to evaluate PFS in accordance with RECIST, version 1.1 (22). PFS was calculated as time from ^{64}Cu -DOTATATE PET/CT to, if any, progression or death from any cause. If no progression or death from any cause occurred within the follow-up interval, the patient was censored at the time of the last available diagnostic imaging. OS was calculated as time from ^{64}Cu -DOTATATE PET/CT to death from any cause. Patients alive at follow-up were censored to the day of follow-up, that is, July 13, 2020.

Statistics

Continuous variables are reported as mean and SEM or as median and range. Kaplan–Meier analysis was used to estimate the median time, with 95% confidence interval (CI), to the endpoint. Uni- and multivariate Cox regression analyses for outcome were performed for the derived PET parameters as continuous and dichotomized (by median) parameters. Use of median total tumor volume and minimum SUV_{mean} as suitable cutoffs was investigated using the R-package “Cutoff Finder” (23). A P value of less than 0.05 was considered statistically significant. R statistical software, version 4.0.0. (R Foundation for Statistical Computing) was used for the analyses.

TABLE 1

Baseline Characteristics of 116 Patients with NENs

Characteristic	Data
Mean age (y)	62.2 (SD, 10.8)
Sex	
Male	64 (55)
Female	52 (45)
Median Ki-67 [†] (%)	5 (range, 1–100)
World Health Organization grade [†]	
G1	27 (23)
G2	79 (68)
G3	4 (3)
Missing	6 (5)
Site of primary	
Small intestine	66 (57)
Pancreas	25 (22)
Cecum	7 (6)
Extrahepatic biliary tract	2 (2)
Gastric	1 (1)
Lung	5 (4)
Unknown primary NEN	10 (9)
Treatment before ⁶⁴ Cu-DOTATATE PET/CT [‡]	
None	15 (13)
Localized	10 (8)
Systemic	43 (37)
Localized and systemic	48 (41)

*Missing for 6 patients.

[†]Patients with lung NENs had Ki-67 < 10% and were accordingly placed in G1 and G2.

[‡]Localized treatment for NENs: surgery (*n* = 52), hepatic artery embolization (*n* = 7), radiofrequency ablation (*n* = 7), or external radiation (*n* = 2). Systemic treatment for NENs: interferon (*n* = 52), somatostatin analog (*n* = 47), chemotherapy (*n* = 48), or peptide receptor radionuclide therapy (*n* = 36).

Data are number followed by percentage in parentheses, unless otherwise indicated. Percentages were rounded and may not add up to 100%.

RESULTS

In total, 128 patients with ⁶⁴Cu-DOTATATE PET/CT were assessed by the semiautomatic tumor delineation method. A median of 5 lesions was delineated per patient (range, 1–78). We excluded 12 patients because they had no lesions above the minimum tumor volume threshold of 1 cm³. The characteristics of the final population (*n* = 116) are given in Table 1.

Semiautomatic Tumor Delineation

The time spent on the entire process of tumor delineation, including manual deletion of physiologic uptake, was 20 min (range, 5–35 min). The volume threshold, 1 cm³, was applied not when the tumor delineation was performed but in the following postprocessing. The shortest time was spent in patients with few lesions, for whom the drawn region of interest encompassing all lesions did not include foci with physiologic uptake. The median patient-specific SUV

TABLE 2

Parameters Obtained by Semiautomatic Total Tumor Delineation on ⁶⁴Cu-DOTATATE PET in 116 Patients

Parameter	Data
SUV _{max}	58.6 (13.4–195)
Minimum SUV _{mean}	14.2 (5.6–56.8)
Total tumor volume (cm ³)	54.9 (1.1–3,840)
Threshold for delineation	8.52 (4.7–14.9)

Data are median followed by range in parentheses.

threshold was 8.58 and was defined from normal liver tissue in most patients (108/116; 93%). In 11 of 12 patients, the interreader comparison showed concordance regarding categorization according to total tumor volume and minimum SUV_{mean}. In 1 patient, the physiologic uptake of the bladder had mistakenly not been removed; hence, the volume was overestimated, leading to a discordant classification.

PET Parameters

The derived total tumor volume and SUV parameters are shown in Table 2. Minimum SUV_{mean} and total tumor volume were both statistically significantly associated with PFS and OS in univariate Cox regression analyses, whereas SUV_{max} was only for PFS (Table 3). In multivariate analyses of minimum SUV_{mean} and total tumor volume as continuous parameters, both remained statistically significantly associated with PFS and OS (Table 4).

PFS and OS

Median PFS was 23 mo (95% CI, 20–31 mo) and median OS was 85 mo (95% CI, 68–113 mo) for the entire patient cohort (*n* = 116). During follow-up, 103 patients (89%) had disease progression and 68 died (59%). Total tumor volume and minimum SUV_{mean} were dichotomized at median values based on analyses of the optimal cut-off for each parameter (Supplemental Fig. 1; supplemental materials are available at <http://jnm.snmjournals.org>). Patients were divided into 4 possible groups: high total tumor volume + low minimum SUV_{mean}, high total tumor volume + high minimum SUV_{mean}, low total tumor volume + low minimum SUV_{mean}, and low total tumor volume + high minimum SUV_{mean}. Representative patient examples from the 4 groups are shown with and without semiautomatic tumor segmentation in Figure 1. Patients in the group with a high total tumor volume + low minimum SUV_{mean} (*n* = 43) had a median PFS of 13 mo (95% CI, 7–21 mo) and a median OS of 31 mo (95% CI, 18–53 mo). For patients in the group with low total tumor volume + high minimum SUV_{mean} (*n* = 43), median PFS was 42 mo (95% CI, 25–80 mo) and median OS was not reached (lower limit of median, 95 mo). Using the group with a high total tumor volume + low minimum SUV_{mean} as the reference group, patients in the group with a low total tumor volume + high minimum SUV_{mean} had a hazard ratio of 0.32 (95% CI, 0.2–0.51) for PFS and 0.24 (95% CI, 0.13–0.43) for OS, both with a *P* value of less than 0.001 (Table 5; Fig. 2). Although not powered for this purpose, exploratorily we assessed the categorization separately in patients with small intestine and pancreatic primary tumors and found a similar prognostic performance (Supplemental Table 1). In comparison, no significant differences were observed between patients with a Ki-67 of less than 3% (*n* = 27) and patients with a Ki-67 of 3%–20% (*n* = 79) in regard to PFS and OS (Supplemental Table 2; Supplemental Fig. 2).

TABLE 3

Univariate Cox Regression Analyses for PFS and OS in 116 Patients

Parameter	Hazard ratio	<i>P</i>
PFS		
SUV _{max}	0.99 (0.99–1.00)	0.049
Minimum SUV _{mean}	0.94 (0.90–0.98)	<0.001
Total tumor volume	1.001 (1.00–1.001)	<0.001
OS		
SUV _{max}	0.99 (0.99–1.00)	0.12
Minimum SUV _{mean}	0.91 (0.86–0.96)	<0.001
Total tumor volume	1.001 (1.001–1.001)	<0.001

All parameters are continuous. Data in parentheses are 95% CIs.

TABLE 4

Multivariate Cox Regression Analyses for PFS and OS in 116 Patients

Parameter	Hazard ratio	<i>P</i>
PFS		
Minimum SUV _{mean}	0.96 (0.92–1.00)	0.03
Total tumor volume	1.001 (1.00–1.001)	<0.01
OS		
Minimum SUV _{mean}	0.94 (0.89–1.00)	0.045
Total tumor volume	1.001 (1.00–1.001)	<0.001

All parameters are continuous. Data in parentheses are 95% CIs.

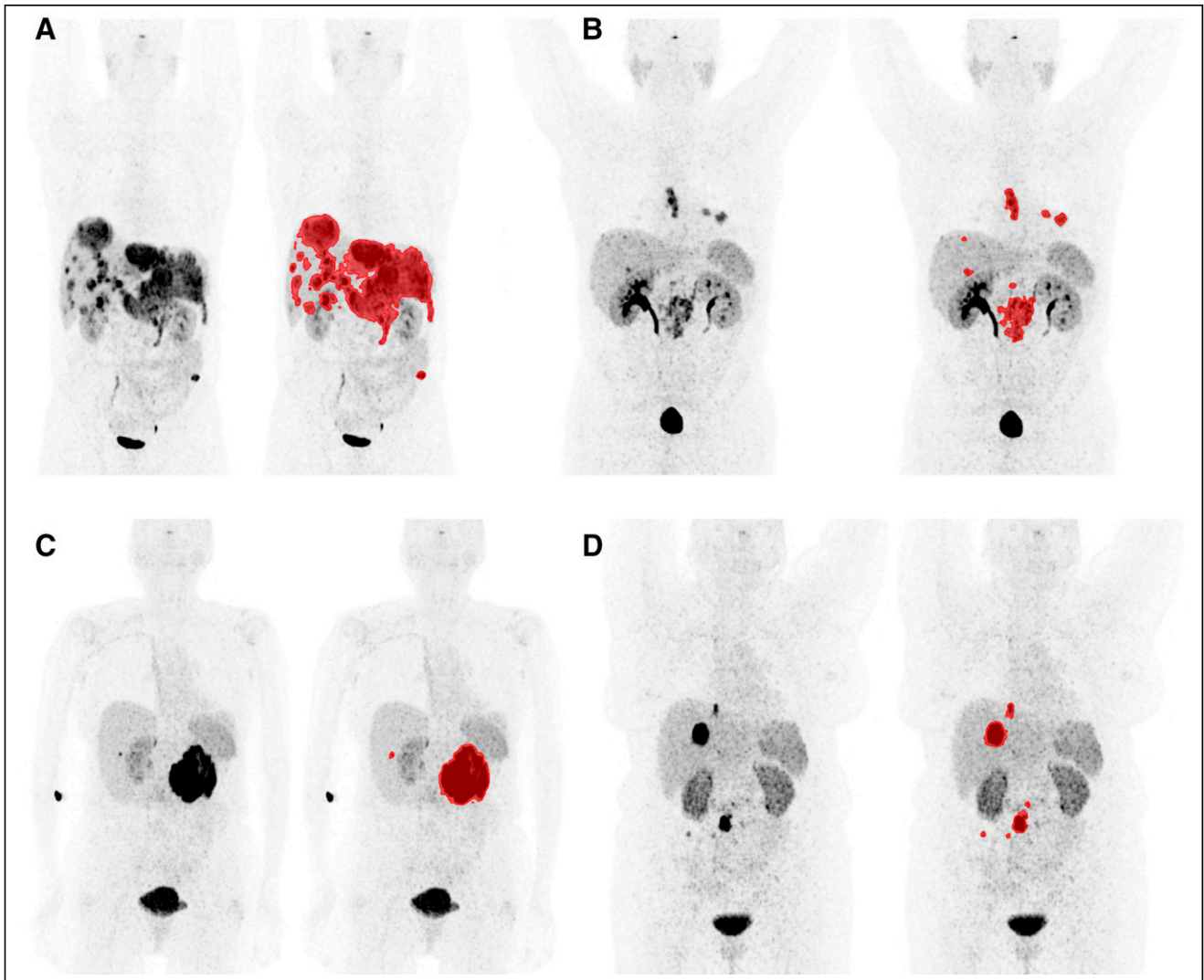


FIGURE 1. Patient examples of classification based on lowest lesion uptake combined with total tumor volume. Maximum-intensity projections are shown without and with delineated tumor volume. Window setting for all images was 0–30. All separate lesions were analyzed individually to obtain minimum SUV_{mean}. (A) Patient in group with high total tumor volume (1,041 cm³) + low minimum SUV_{mean} (9.6); OS, 17 mo; PFS, 11 mo. (B) Patient in group with low total tumor volume (54 cm³) + low minimum SUV_{mean} (13.1); OS, 51 mo; PFS, 42 mo. (C) Patient in group with high total tumor volume (415 cm³) + high minimum SUV_{mean} (25.3); OS, 68 mo; PFS, 34 mo. (D) Patient in group with low total tumor volume (45 cm³) + high minimum SUV_{mean} (15); OS, 118 mo; PFS, 80 mo.

TABLE 5

Univariate Cox Regression Analyses for PFS and OS in 116 Patients

Group	Hazard ratio	P
PFS		
VhSI (n = 43)	Reference	—
VhSh (n = 15)	0.51 (0.28–0.94)	0.03
VISI (n = 15)	0.58 (0.32–1.08)	0.08
VISh (n = 43)	0.32 (0.20–0.51)	<0.001
OS		
VhSI (n = 43)	Reference	—
VhSh (n = 15)	0.43 (0.21–0.90)	0.02
VISI (n = 15)	0.27 (0.12–0.61)	<0.01
VISh (n = 43)	0.24 (0.13–0.43)	<0.001

VhSI = high total tumor volume + low minimum SUV_{mean}; VhSh = high total tumor volume + high minimum SUV_{mean}; VISI = low total tumor volume + low minimum SUV_{mean}; VISh = low total tumor volume + high minimum SUV_{mean}.
 Patients with high total tumor volume and low minimum SUV_{mean} are reference. Data in parentheses are 95% CIs.

DISCUSSION

The major finding of our study was that the prognostic value of ⁶⁴Cu-DOTATATE PET in patients with NENs could be greatly improved by evaluating the lowest lesion uptake rather than the highest. This finding is in accordance with our hypothesis and fits well into somatostatin receptor density’s being a surrogate of differentiation, that is, lower density in more dedifferentiated and aggressive tumors. We furthermore present a novel combined classification of total tumor volume and lowest lesion uptake from ⁶⁴Cu-DOTATATE PET to incorporate previous reports that tumor volume derived

from SRI (10–14) is associated with prognosis in patients with NENs. Applying the combination of total tumor volume and lowest lesion uptake, we classified patients into 4 groups, with patients in the group with a high total tumor volume + low minimum SUV_{mean} having the poorest prognosis in regard to PFS and OS.

We and others have reported on the prognostic ability of lesion SUV_{max} from either ⁶⁴Cu-DOTATATE (6) or ⁶⁸Ga-DOTATATE/DOTANOC (24–26). A limitation to that metric, besides concerns about the influence of image noise on single-pixel SUV_{max} (27), is the fact that prognostication then is based on the lesion with the highest uptake, that is, with greater somatostatin receptor density. One previous study of 30 patients with NENs investigating prognostication based on the lesion with the lowest uptake did, however, fail to show an association between lower uptake and higher risk of progressive disease (26). Furthermore, total lesion somatostatin receptor expression (the product of tumor volume and SUV_{mean}) has been proposed (10). However, the results we present contradict this concept. The effect of total tumor volume and SUV_{mean} have an opposite direction, and a high “total lesion activity” in SRI may be seen in patients with a low tumor burden and a high SUV_{mean} or in patients with a high tumor burden and a low SUV_{mean}. As presented, two such patients would be expected to have a different prognosis.

A prerequisite to analyzing total tumor volume and minimum SUV_{mean} is tumor segmentation. A standardized semiautomatic method for PET-guided segmentation in patients with NENs has not been reported previously. We therefore used a standardized patient-specific cutoff to delineated lesions on the basis of the method described for ¹⁸F-FDG (19). Recently, several papers have described the prognostic implications of tumor volume derived from ⁶⁸Ga-DOTATATE (10–12) or ⁶⁸Ga-DOTATOC (13,14), but not for ⁶⁴Cu-DOTATATE. To obtain tumor volume, different strategies were used: manual delineation of lesions including areas with either 41% or 50% of lesion SUV_{max} or semiautomatic delineation with individual SUV_{max} threshold based on agreement between anatomic and functional lesion delineation. However, none of the studies reported the time spent on segmentation of tumors (8–14). In the present study, the time spent was approximately 20 min per patient, although less

time (down to 5 min) was needed when areas of physiologic uptake (kidney, urinary bladder, and spleen) could be avoided because of the tumor location. Patients were concordantly grouped by the total tumor volume/minimum SUV_{mean} classification in all but 1 patient in the interreader analysis. The presented semiautomatic segmentation scheme may be feasible for clinical translation; however, faster segmentation is desirable. One approach would be to minimize the need for manual deletion of physiologic uptake by use of anatomic data gained from the CT scan. This approach has been demonstrated for prostate cancer using ⁶⁸Ga-PSMA PET (28). An added gain would be that of organ-specific tumor burden—for example, tumor burden in liver or bone. Subclassification according to tumor location may further enhance the prognostic implication of total tumor volume; for example, it could be speculated that patients with mainly liver metastases have a different prognosis from patients with mainly bone metastases.

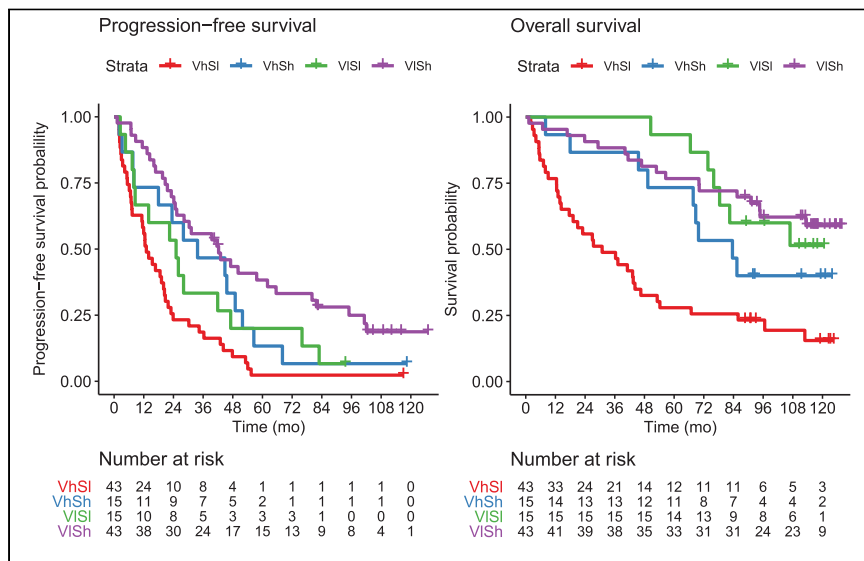


FIGURE 2. Kaplan-Meier plots of PFS and OS for patients grouped by total tumor volume and minimum SUV_{mean}. VhSh = high total tumor volume + high minimum SUV_{mean}; VhSI = high total tumor volume + low minimum SUV_{mean}; VISh = low total tumor volume + high minimum SUV_{mean}; VISI = low total tumor volume + low minimum SUV_{mean}.

This study had some limitations. The threshold used to delineate lesions was based on PERCIST, as no standardized semiautomated criteria have been suggested for SRI PET. To limit the partial-volume effect, only lesions greater than 1 cm³ were used for analysis of SUV. A larger required lesion size could have further limited the partial-volume effect, but at the cost of excluding a larger proportion of the lesions, hence potentially excluding more patients because of small lesions. Using the 1 cm³ cutoff, 12 of 128 patients were excluded, which limits the general use. The results may not translate directly to SRI PET with ⁶⁸Ga because of the better resolution of ⁶⁴Cu-based imaging (a 4-fold shorter positron range) (29).

CONCLUSION

A standardized semiautomatic tumor segmentation scheme was applied to obtain total tumor volume and minimum lesion SUV_{mean} from ⁶⁴Cu-DOTATATE PET images of patients with NENs. By use of the lowest lesion uptake, rather than the highest, results from ⁶⁴Cu-DOTATATE PET were significantly associated with both PFS and OS. Furthermore, patients could be classified into 4 groups with high or low total tumor volume and high or low minimum SUV_{mean}, with patients with a high total tumor volume and low minimum SUV_{mean} having the poorest prognosis.

DISCLOSURE

Andreas Kjaer and Ulrich Knigge are inventors on a patent application: “PET Tracer for Imaging of Neuroendocrine Tumors” (WO 2013029616 A1). This project received funding from the European Union’s Horizon 2020 research and innovation program under grants 670261 (ERC Advanced Grant) and 668532 (Click-It), the Lundbeck Foundation, the Novo Nordisk Foundation, the Innovation Fund Denmark, the Danish Cancer Society, the Arvid Nilsson Foundation, the Svend Andersen Foundation, the Neye Foundation, the Research Foundation of Rigshospitalet, the Danish National Research Foundation (grant 126), the Research Council of the Capital Region of Denmark, the Danish Health Authority, the John and Birthe Meyer Foundation, and Research Council for Independent Research. No other potential conflict of interest relevant to this article was reported.

KEY POINTS

QUESTION: Is the prognostic capability of ⁶⁴Cu-DOTATATE PET in patients with NENs improved by using total tumor segmentation to identify the lesion with lowest uptake compared with maximal uptake?

PERTINENT FINDINGS: Minimum SUV_{mean} as a measure of the lowest lesion uptake was strongly associated with both OS and PFS. This was not the case for maximal lesion uptake. We present a standardized semiautomatic tumor segmentation scheme and use it to define a novel classification combining total tumor volume and minimum SUV_{mean}. Patients with a high total tumor volume and low minimum SUV_{mean} have a significantly worse prognosis than other patients do.

IMPLICATIONS FOR PATIENT CARE: On the basis of combining total tumor volume and minimum SUV_{mean} in ⁶⁴Cu-DOTATATE PET, patients with NENs may be classified into 4 groups and stratified with different risks of progressive disease and death. The classification may aid in clinical treatment decisions.

ACKNOWLEDGMENTS

We thank the staff at the Department of Clinical Physiology, Nuclear Medicine, and PET for help in providing the PET tracer and in performing the PET/CT studies.

REFERENCES

1. WHO Classification of Tumours Editorial Board. *Digestive System Tumours*. 5th ed. International Agency for Research on Cancer; 2019:16–19.
2. Couvelard A, Deschamps L, Ravaud P, et al. Heterogeneity of tumor prognostic markers: a reproducibility study applied to liver metastases of pancreatic endocrine tumors. *Mod Pathol*. 2009;22:273–281.
3. Miller HC, Drymoussis P, Flora R, Goldin R, Spalding D, Frilling A. Role of Ki-67 proliferation index in the assessment of patients with neuroendocrine neoplasias regarding the stage of disease. *World J Surg*. 2014;38:1353–1361.
4. Shi H, Zhang Q, Han C, Zhen D, Lin R. Variability of the Ki-67 proliferation index in gastroenteropancreatic neuroendocrine neoplasms: a single-center retrospective study. *BMC Endocr Disord*. 2018;18:51.
5. Yang Z, Tang LH, Klimstra DS. Effect of tumor heterogeneity on the assessment of Ki67 labeling index in well-differentiated neuroendocrine tumors metastatic to the liver: implications for prognostic stratification. *Am J Surg Pathol*. 2011;35:853–860.
6. Carlsen EA, Johnbeck CB, Binderup T, et al. ⁶⁴Cu-DOTATATE PET/CT and prediction of overall and progression-free survival in patients with neuroendocrine neoplasms. *J Nucl Med*. 2020;61:1491–1497.
7. Lim SM, Kim H, Kang B, et al. Prognostic value of ¹⁸F-fluorodeoxyglucose positron emission tomography in patients with gastric neuroendocrine carcinoma and mixed adenoneuroendocrine carcinoma. *Ann Nucl Med*. 2016;30:279–286.
8. Kim HS, Choi JY, Choi DW, et al. Prognostic value of volume-based metabolic parameters measured by ¹⁸F-FDG PET/CT of pancreatic neuroendocrine tumors. *Nucl Med Mol Imaging*. 2014;48:180–186.
9. Chan DL, Bernard EJ, Schembri G, et al. High metabolic tumour volume on ¹⁸F-fluorodeoxyglucose positron emission tomography predicts poor survival from neuroendocrine neoplasms. *Neuroendocrinology*. 2020;110:950–958.
10. Abdulrezzak U, Kurt YK, Kula M, Tutus A. Combined imaging with ⁶⁸Ga-DOTATATE and ¹⁸F-FDG PET/CT on the basis of volumetric parameters in neuroendocrine tumors. *Nucl Med Commun*. 2016;37:874–881.
11. Toriihara A, Baratto L, Nobashi T, et al. Prognostic value of somatostatin receptor expressing tumor volume calculated from ⁶⁸Ga-DOTATATE PET/CT in patients with well-differentiated neuroendocrine tumors. *Eur J Nucl Med Mol Imaging*. 2019;46:2244–2251.
12. Tirosh A, Papadakis GZ, Millo C, et al. Prognostic utility of total ⁶⁸Ga-DOTATATE-avid tumor volume in patients with neuroendocrine tumors. *Gastroenterology*. 2018;154:998–1008.e1.
13. Ohnona J, Nataf V, Gauthier M, et al. Prognostic value of functional tumor burden on ⁶⁸Ga-DOTATOC PET/CT in patients with pancreatic neuroendocrine tumors. *Neoplasma*. 2019;66:140–148.
14. Pauwels E, Van Binnebeek S, Vandecaveye V, et al. Inflammation-based index and ⁶⁸Ga-DOTATOC PET-derived uptake and volumetric parameters predict outcome in neuroendocrine tumor patients treated with ⁹⁰Y-DOTATOC. *J Nucl Med*. 2020;61:1014–1020.
15. Pfeifer A, Knigge U, Binderup T, et al. ⁶⁴Cu-DOTATATE PET for neuroendocrine tumors: a prospective head-to-head comparison with ¹¹¹In-DTPA-octreotide in 112 patients. *J Nucl Med*. 2015;56:847–854.
16. Johnbeck CB, Knigge U, Loft A, et al. Head-to-head comparison of ⁶⁴Cu-DOTATATE and ⁶⁸Ga-DOTATOC PET/CT: a prospective study of 59 patients with neuroendocrine tumors. *J Nucl Med*. 2017;58:451–457.
17. Knigge U, Capdevila J, Bartsch DK, et al. ENETS consensus recommendations for the standards of care in neuroendocrine neoplasms: follow-up and documentation. *Neuroendocrinology*. 2017;105:310–319.
18. Pfeifer A, Knigge U, Mortensen J, et al. Clinical PET of neuroendocrine tumors using ⁶⁴Cu-DOTATATE: first-in-humans study. *J Nucl Med*. 2012;53:1207–1215.
19. Wahl RL, Jacene H, Kasamon Y, Lodge MA. From RECIST to PERCIST: evolving considerations for PET response criteria in solid tumors. *J Nucl Med*. 2009;50(suppl 1):122S–150S.
20. Loft M, Carlsen EA, Johnbeck CB, et al. ⁶⁴Cu-DOTATATE PET in patients with neuroendocrine neoplasms: prospective, head-to-head comparison of imaging at 1 hour and 3 hours after injection. *J Nucl Med*. 2021;62:73–80.
21. Soret M, Bacharach SL, Buwat I. Partial-volume effect in PET tumor imaging. *J Nucl Med*. 2007;48:932–945.

22. Eisenhauer EA, Therasse P, Bogaerts J, et al. New response evaluation criteria in solid tumours: revised RECIST guideline (version 1.1). *Eur J Cancer*. 2009;45:228–247.
23. Budczies J, Klauschen F, Sinn BV, et al. Cutoff Finder: a comprehensive and straightforward Web application enabling rapid biomarker cutoff optimization. *PLoS One*. 2012;7:e51862.
24. Ambrosini V, Campana D, Polverari G, et al. Prognostic value of ^{68}Ga -DOTANOC PET/CT SUVmax in patients with neuroendocrine tumors of the pancreas. *J Nucl Med*. 2015;56:1843–1848.
25. Campana D, Ambrosini V, Pezzilli R, et al. Standardized uptake values of ^{68}Ga -DOTANOC PET: a promising prognostic tool in neuroendocrine tumors. *J Nucl Med*. 2010;51:353–359.
26. Koch W, Auernhammer CJ, Geisler J, et al. Treatment with octreotide in patients with well-differentiated neuroendocrine tumors of the ileum: prognostic stratification with Ga-68-DOTA-TATE positron emission tomography. *Mol Imaging*. 2014;13:1–10.
27. Lodge MA, Chaudhry MA, Wahl RL. Noise considerations for PET quantification using maximum and peak standardized uptake value. *J Nucl Med*. 2012;53:1041–1047.
28. Seifert R, Herrmann K, Kleesiek J, et al. Semiautomatically quantified tumor volume using ^{68}Ga -PSMA-11 PET as a biomarker for survival in patients with advanced prostate cancer. *J Nucl Med*. 2020;61:1786–1792.
29. Conti M, Eriksson L. Physics of pure and non-pure positron emitters for PET: a review and a discussion. *EJNMMI Phys*. 2016;3:8.